Nanoscale

Dynamic Article Links

Cite this: *Nanoscale*, 2012, **4**, 897

www.rsc.org/nanoscale

PAPER

A computational and experimental investigation of the mechanical properties of single ZnTe nanowires†

Keivan Davami,[a] Bohayra Mortazavi,‡[bc] Hessam M. Ghassemi,‡[d] Reza S. Yassar,[d] Jeong-Soo Lee,*[a] Yves Rémond[c] and M. Meyyappan*[ae]

Received 27th October 2011, Accepted 21st November 2011
DOI: 10.1039/c2nr11593j

One-dimensional nanostructures such as ZnTe, CdTe, Bi_2Te_3 and others have attracted much attention in recent years for their potential in thermoelectric devices among other applications. A better understanding of their mechanical properties is important for the design of devices. A combined experimental and computational approach has been used here to investigate the size effects on the Young's modulus of ZnTe nanowires (NWs). The mechanical properties of individual ZnTe nanowires in a wide diameter range (50–230 nm) were experimentally measured inside a high resolution transmission electron microscope using an atomic force microscope probe with the ability to record *in situ* continuous force–displacement curves. The *in situ* observations showed that ZnTe NWs are flexible nanostructures with the ability to withstand relatively high buckling forces without becoming fractured. The Young's modulus is found to be independent of nanowire diameter in the investigated range, in contrast to reported results for ZnO NWs and carbon nanotubes where the modulus increases with a decrease in diameter. Molecular dynamics simulations performed for nanowires with diameters less than 20 nm show limited size dependence for diameters smaller than 5 nm. The surface atoms present lower Young's modulus according to the simulations and the limited size dependency of the cylindrical ZnTe NWs is attributed to the short range covalent interactions.

1. Introduction

Characterization of mechanical properties of nanostructured materials is a challenge due to difficulties in positioning, clamping, applying forces, and reading the output force or displacement, all attributed to the minuscule size of these structures.[1] Consequently, these measurements are rare in the literature and there is not much information about the mechanical properties of inorganic nanowires, particularly in comparison with carbon nanotubes.[2–6] The inorganic nanowires have been receiving significant attention for applications in electronics, optoelectronics, photovoltaics, batteries, and numerous others.[7] Therefore, novel and reliable experimental methods are needed for evaluating the mechanical properties of nanowires (NWs).

There are several techniques for the characterization of nanostructures in the literature, each with its own merits and drawbacks. One of the common methods involves the use of atomic force microscopy (AFM) to bend a NW anchored at one end of the substrate with the other end being free. The elastic modulus and other mechanical properties of the NWs can be calculated using the force deflection data. Wong *et al.* used this method to obtain the elastic modulus, strength, and toughness of nanorods and nanotubes.[8] Wu *et al.* used an AFM tip to bend a NW suspended in the middle and clamped at the two ends.[9] Their results showed that the Young's modulus of a gold NW is not dependent on the diameter while the strength increases with a decrease in NW diameter. While AFM-based approaches are relatively simple and the sample preparation can be done readily, the disadvantage includes the inability to observe the NW structure while the force is being applied.

Using a transmission electron microscopy (TEM) setup helps to overcome the above problem and it is possible to measure the mechanical properties of nanostructures inside a TEM. In one method, a NW is vibrated using an alternating electrostatic field at a known frequency and the dynamic response inside the TEM is then analyzed. The amplitude and phase of the dynamic response

[a]*Department of IT convergence Engineering, Pohang University of Science and Technology (POSTECH), Pohang, South Korea. E-mail: ljs6951@postech.ac.kr*
[b]*Centre de Recherche Public Henri Tudor, Department of Advanced Materials and Structures, 66, rue de Luxembourg BP 144, L-4002 Esch/Alzette, Luxembourg*
[c]*Institut de Mécanique des Fluides et des Solides, University of Strasbourg/CNRS, 2 Rue Boussingault, 67000 Strasbourg, France*
[d]*Department of Mechanical Engineering—Engineering Mechanics, Michigan Technoological University, Houghton, MI, 49931, USA*
[e]*NASA Ames Research Center, Moffett Field, CA, 94035, USA. E-mail: m.meyyappan@nasa.gov*

† Electronic supplementary information (ESI) available. See DOI: 10.1039/c2nr11593j

‡ These authors contributed equally.

are used to calculate the Young's modulus of the NW.[10–12] This method was used for the mechanical characterization of multi-walled carbon nanotubes (MWCNTs) to report that the elastic bending modulus as a function of diameter decreases intensely (from about 1 to 0.1 TPa) when the diameter increases from 8 to 40 nm.[3] A second approach benefits from a specially designed MEMS (microelectromechanical system) device suitable for use in scanning electron microscopy (SEM) and TEM for mechanical property measurement of one-dimensional structures.[1] This approach has been used for NWs and nanoscale thin films;[13] for example, an Young's modulus of 155 ± 5 GPa and failure strength of 0.7 GPa were obtained for polysilicon beams. In the case of [0001] oriented ZnO NWs, an increase of about 20 GPa in Young's modulus was observed when the diameter of NWs was decreased from 80 to 20 nm.[14] The Young's modulus was shown to be the same as the bulk value for thicker ZnO NWs and the results were also confirmed using molecular dynamics (MD) simulations for NWs thinner than 20 nm.

Here we investigate the mechanical properties of individual thin and thick ZnTe NWs (50–230 nm) experimentally using an integrated TEM-AFM holder, with the ability to record *in situ* continuous force–displacement curves. The displacement is controlled using a piezo-driven system with a precision of 1 nm in *X*, *Y* and *Z* directions. The measurement is done in a vacuum TEM chamber using AFM Nanofactory holders. In addition, we have calculated the mechanical properties of thinner ZnTe NWs (2.5–20 nm) using MD simulations. ZnTe and CdTe nanowires are useful for thermoelectric refrigeration and power generation, detectors and other optoelectronic applications[7] and understanding their properties is critical to advancing application development.

2. Experimental procedure

The *in situ* experiments were conducted using an AFM Nanofactory probe that was operated inside a JEOL JEM-4000FX TEM at 200 kV. The ZnTe NWs were grown on silicon substrates covered with a 2 nm gold film *via* a VLS (vapor–liquid–solid) method. Details of the growth process and optimum conditions to obtain NWs over nanoribbons and tapered wires can be found in ref. 15. Individual NWs were completely analyzed using SEM, HRTEM, and energy dispersive X-ray (EDX) spectroscopy prior to starting the mechanical property measurements. Fig. 1 shows a schematic of the measurement setup used in this study. Individual ZnTe NWs were attached on a gold wire by light mechanical scratching on the silicon substrate containing the as-grown nanowires. Individual NWs stick to the gold wire as a result of van der Waals force. The Au wire was then fixed on the Au hat, which sits on the sapphire ball. The piezo-driven holder allows nanometre motion of the sample toward the AFM tip by applying a frictional force between the hat legs and the sapphire ball. The sample position can be adjusted with a precision of 1 nm in *X*, *Y* and *Z* directions. An axial compression was applied after positioning the nanowire and the force–displacement curves were recorded.

3. Results and discussion

Fig. 2a is an SEM image showing a mat of ZnTe nanowires 25–100 nm diameter and several microns long. Fig. 2b shows an individual NW of 25.9 nm in diameter and the HRTEM image in Fig. 2c indicates the presence of an amorphous oxide layer on the NW surface. The EDS results in Fig. 2d confirm that the stoichiometric ratio of Zn : Te to be close to 1 : 1. The diffraction pattern presented in Fig. 2e reveals the single crystal structure of the NW. Detailed structural analysis of ZnTe nanowires can be found in our earlier work in ref. 15.

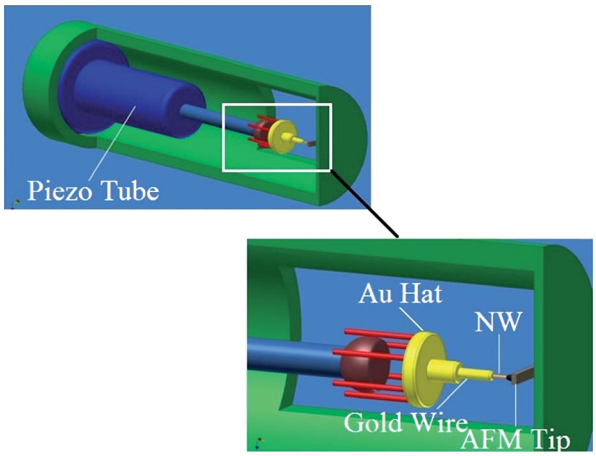

Fig. 1 A schematic of the *in situ* AFM setup inside the TEM.

Fig. 3a shows an individual ZnTe NW between the AFM probe and the gold wire. At this initial stage, there is no sign of bending throughout the length of the NW. Fig. 3b–d show the NW bending to the right under the applied force and Fig. 3e–g show the same NW bending to the left during the second cycle of the applied force (the corresponding video can be found in the ESI†). Note that the amount of applied force is not changed as plotted in Fig. 3h. Using the maximum applied forces in the *F*–*D* curves, the Young's modulus of NW can be calculated based on the Euler's formula assuming that both ends are fixed, where the maximum applied force is $F_{\text{Euler}} = n\pi^2 EI/L^2$. Here, *L* is the length of the NW between the two contacts, *E* is the elastic modulus, *I* is the moment of inertia for a nanowire with circular cross-section $I = \pi d^4/64$, and *d* is the diameter. The value of the constant *n* depends on the conditions of the end support of the NW. Here, the NW can be considered to have both ends pinned with the ability to rotate[16] since the nanowire is not glued or clamped at the ends but kept by the van der Waals force between the gold wire and the probe; the value of *n* for such a configuration can be taken as 1.0.[17]

Fig. 4 reveals the reproducibility of the force–displacement measurements for a NW with $d = 165$ nm and $L = 10$ μm for six sequential runs. The overlap of the curves confirms the considerable reproducibility of the experimental results. No plastic deformation was observed in the nanowire after each run. Fig. 5 shows the values of the measured elastic modulus of ZnTe NWs along with those from MD simulations (details will be discussed later). The elastic modulus of the ZnTe NW does not seem to change with diameter in the 40–250 nm range investigated here, and it is approximately 63.0 ± 6.0 GPa, slightly lower than 70 GPa reported for [111] oriented nanocrystalline ZnTe thin films.[18] The modulus of bulk ZnTe in the [111] direction (growth direction of ZnTe NWs) can be extracted for comparison as follows. Yamada *et al.*[19] obtained the elastic constants of ZnTe

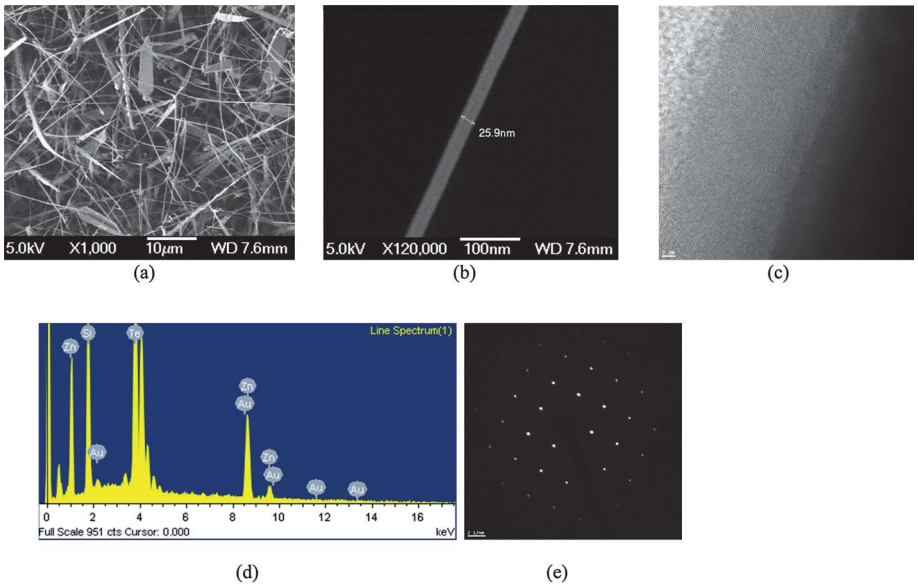

Fig. 2 (a) SEM image of a mat of ZnTe nanowires on a silicon substrate, (b) SEM image of a single ZnTe nanowire, (c) HRTEM image of a ZnTe nanowire, (d) EDS analysis of the ZnTe nanowire, and (e) diffraction pattern of the NW sample.

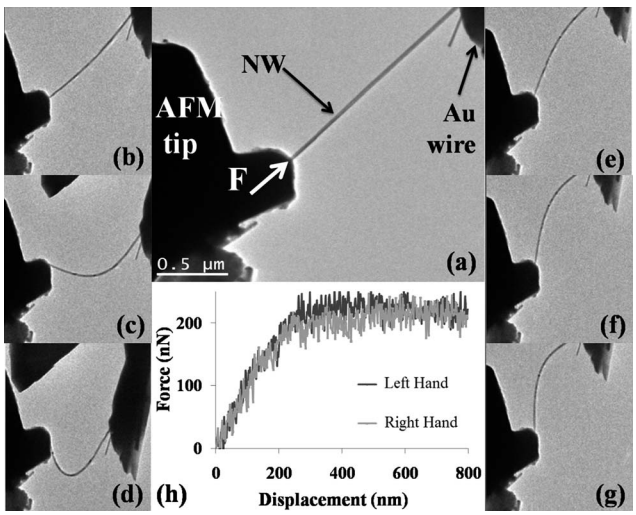

Fig. 3 (a) An individual ZnTe NW before the bending experiment in contact with the AFM tip and gold wire, with associated forces. (b–d) Video shot series of rightward bending of the NW. (e–g) Video shot series of leftward bending of the same NW. (h) Plots of the force–displacement of both the rightward and leftward bending of the NW indicating that the amounts of force and displacement are the same.

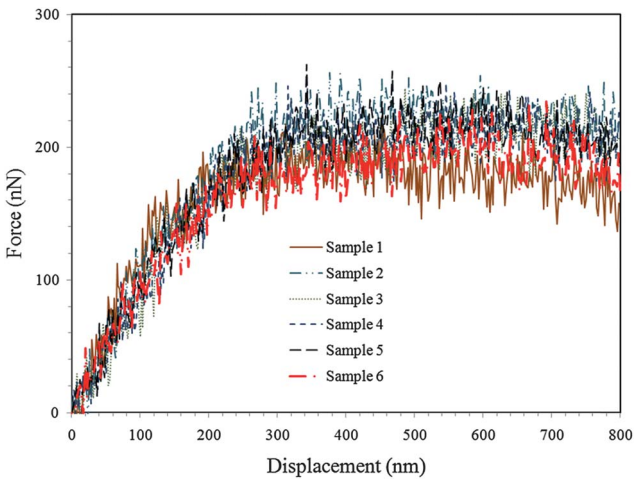

Fig. 4 Reproducibility of the force–displacement curves for a NW with a diameter of 165 nm and length of 10 μm for six sequential runs.

crystals from Brillouin scattering spectra with 90-scattering geometry at room temperature as $C_{11} = 7.22 \pm 0.02$, $C_{12} = 4.09 \pm 0.06$ and $C_{44} = 3.08 \pm 0.03$ in units of 10^{10} N m^{-2}. Lee[20] used an ultrasonic pulse-echo method and reported elastic constants for ZnTe as $C_{11} = 7.11 \pm 0.03$, $C_{12} = 4.07 \pm 0.04$ and $C_{44} = 3.13 \pm 0.02$ in units of 10^{10} N m^{-2}. Considering the [111] growth direction of our NWs, the Young's modulus of bulk ZnTe may be calculated from the following relation:[21]

$$E'_{<111>} = \frac{1}{3}(C_{11} + 2C_{12} + 4C_{44}) - \frac{2}{9}\frac{(C_{11} + 2C_{12} - 2C_{44})^2}{(C_{11} + C_{12} + 2C_{44})}$$

This provides an elastic modulus of 81.6 GPa for bulk ZnTe in the [111] direction and it is noted that this relation has been found to overpredict the modulus values.[21]

As seen in Fig. 5, the measured elastic modulus of ZnTe NWs is independent of size in the range investigated. In contrast, Asthana *et al.*[22] showed that the Young's modulus for ZnO NWs increases from ~150 GPa to 249 GPa when the NW diameter decreases from 400 to 40 nm; the Young's modulus is 147.3 GPa for thicker nanowires which is close to that of bulk ZnO. Agrawal *et al.*[14] reported an increase in elastic modulus from 140 GPa to 160 GPa for ZnO NWs when the diameter decreases from 80 to 20 nm, with the modulus approaching bulk value (~140 GPa) for large diameter wires. Xu *et al.*[23] also obtained similar results for ZnO nanowires except for a peak modulus of 170 GPa for 20 nm diameter. The observed size effect in ZnO NWs is attributed to the surface reconstruction together with

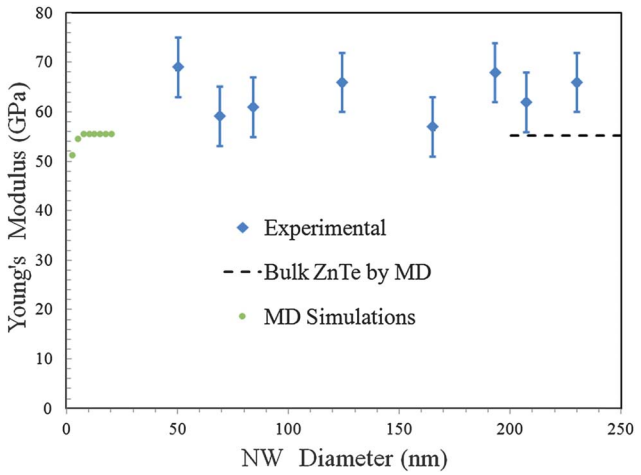

Fig. 5 Variation of the Young's modulus with wire diameter obtained by MD simulation and experiments. The Young's modulus of bulk ZnTe from MD simulation is also shown.

long ionic interaction[14] while such a behavior in metallic NWs is due to the intrinsic compressive state of the NWs at equilibrium.[24,25] The smaller metallic NWs have a higher surface to volume ratio, and the larger extent of contraction causes higher compressive strain at equilibrium leading to a higher Young's modulus.[26] Simulations by Liang *et al.*[27] and Park *et al.*[21] suggest that the level of size dependency of elastic modulus in silicon and copper nanowires is also influenced by the crystallographic loading direction. The size dependency in both cases appears to occur at significantly reduced diameters below 2.5 nm. In the case of copper, the [111] direction shows the least size dependency. Further discussion on size dependency for ZnTe nanowires will be provided later with the aid of the simulation results.

The maximum bending angle for a material in the absence of any dislocation generation is given by $\alpha = 2s/d$, where s is the critical bonding length before the bond breaks and d is the thickness of the material.[28] Nanowires with small diameters can exhibit high bending angles before the initiation of failure. For example, the bending angle of a ZnTe NW with a diameter of 50 nm is 10 000 more than that for a thin wire of ZnTe with a thickness of 0.5 mm. A similar ultrahigh flexibility was observed for SiNWs by Hsin *et al.*[28] who suggested that a change in crystallinity might be the reason for extreme flexibility in addition to the size effect.

We could not measure the Young's modulus of NWs thinner than ~40 nm experimentally, since they act like a spring due to the high flexibility and it was difficult to keep them between the gold wire and the AFM tip. Also, the deflection force of the NW was lower than the resolution of the AFM sensor. As a result, in the case of NWs smaller than 40 nm, all that was recorded were some irregular fluctuations in the force when the displacement was applied. Typically, force measurements in the literature are for the range of 50 to 400 nm diameter nanowires[9,10,12,14,22,23] for similar reasons as mentioned above, with an exception of 20 nm for ZnO nanowires.[14] Therefore, we performed classical Molecular Dynamics (MD) simulations for the prediction of ZnTe NW mechanical properties for nanowires with diameter less than 20 nm, using LAMMPS (Large-Scale Atomic/Molecular Massively Parallel Simulator),[29] developed at Sandia National Laboratories. The interactions in the ZnTe crystals were introduced using the Tersoff's potential with a set of parameters proposed by Kanoun *et al.*[30] This potential has been successfully used by Wang and Chu[31] for the evaluation of temperature-dependent thermal conductivity of bulk ZnTe using the equilibrium molecular dynamics method. The length of the specimen is considered to be twice its diameter in the simulations. A time increment of 1 fs (10^{-15} of a second) was used in the simulations and a periodic boundary condition was used in the loading direction. The loading condition was applied by extending the simulation box along the loading direction with a constant engineering strain rate. As in the experiments, the MD model was constructed in a way that the loading was done along the [111] growth direction for the ZnTe nanowires.[15] The engineering strain at each time step was calculated by multiplying the total time of the deformation process by the loading strain rate. By calculating the virial stresses in the loading direction at each strain level, we could plot the engineering stress–strain response. The elastic modulus of the ZnTe NW was obtained by calculating the slope of the stress–strain relation. Prior to application, the specimen was left to relax to zero stress in the loading direction using constant pressure–temperature (*i.e.* NPT ensemble) by means of the Nosé–Hoover barostat and thermostat method.[32]

As a result of a considerably small time increment in the MD modeling, there are always computational limitations in performing a tensile test with strain rates close to those experimentally available. That is why the tensile tests are usually performed at considerably high strain rates, in the order of 10^{10} s^{-1}. Since the deformation of materials at these high strain rates may be dominated by the temperature effect, we used the Nosé–Hoover thermostat method to control the temperature fluctuations to be around 300 K during the loading process. To ensure the strain rate dependency of the reported values, we performed the MD simulations for a ZnTe NW with a diameter of 5 nm at different strain rates ranging from 10^{11} to 10^{8} s^{-1}. The acquired stress–strain relation for three different strain rates is plotted in Fig. 6a. The stress–strain relation has a linear pattern which continues up to the ultimate tensile strength. Interestingly, the linear part of the relation corresponding to the elastic modulus presents a considerably high level of strain rate independency. The ultimate tensile strength of the NW decreases with the loading strain rate. From these observations, we could predict the stress–strain relation of the ZnTe NW at negligible strain rates by fitting an exponential curve to 11 sets of ultimate strength *vs.* strain rate data and extrapolating the acquired curve to a strain rate of zero (also shown in Fig. 6a). Thus, we predict an ultimate strength of around 6.7 GPa for the static tensile loading conditions. The specimen is also found to present more ductile failure behavior with an increase in strain rate. At high strain rates (Fig. 6a, 1×10^{10} s^{-1}), the load-bearing ability of the specimen declines in a gradual pattern after the specimen reaches the ultimate strength. However, a sharper decrease in stress is seen after the ultimate strength point by decreasing the strain rates. We performed further MD simulations using a strain rate of 2×10^{9} s^{-1}, due to computational efficiency as well as to present a brittle deformation process close to those at lower strain rates.

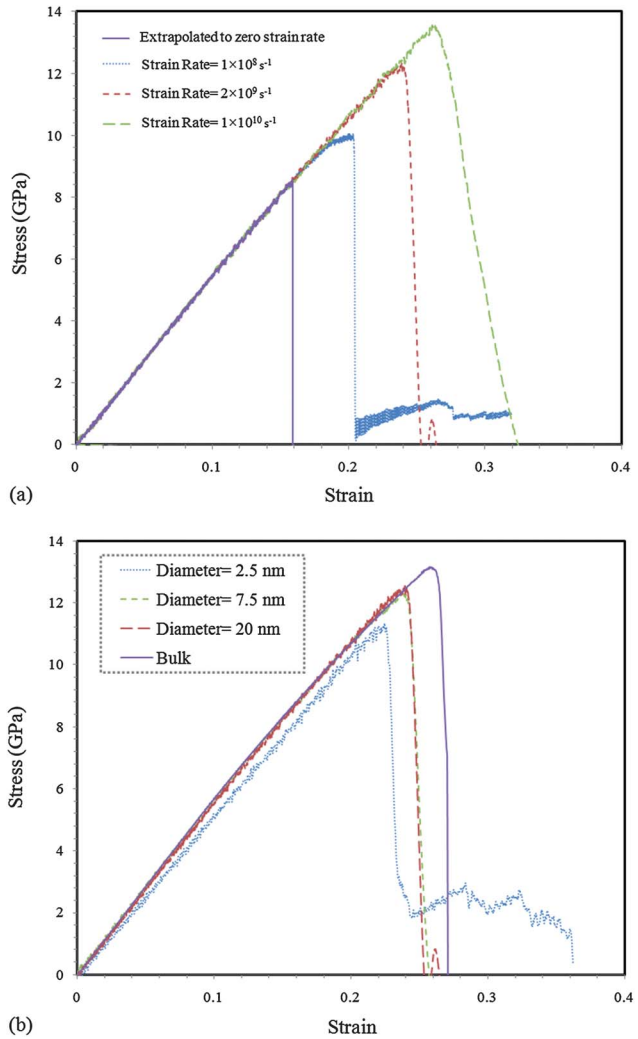

Fig. 6 (a) The strain rate dependency of the stress–strain relation of a 5 nm dia. ZnTe NW and (b) the engineering stress–strain relation for nanowires of different diameters.

The MD simulations were repeated for NWs with different diameters from 2.5 to 20 nm in 2.5 nm steps and the corresponding stress–strain relations are plotted in Fig. 6b along with the results for bulk ZnTe. Simulations of larger diameters used in the experimental study are prohibitively computational-intensive. The stress–strain relation of bulk ZnTe was evaluated by development of a squared section ZnTe specimen, where the periodic boundary conditions were also applied in the section and simulation boxes were set to alter to reach zero stress in these directions by the NPT method. Since the linear part of the stress–strain relation for the 7.5 and 20 nm NW cases overlaps with that of bulk ZnTe, we could conclude that size dependency is not observed for NWs with diameters larger than 7.5 nm and that ZnTe presents limited size dependency only for diameters smaller than 5 nm. Based on the current study, we obtain an elastic modulus of around 55.5 ± 1 GPa for ZnTe NWs with diameters larger than 7.5 nm (see Fig. 5). This is lower than the experimental results discussed earlier and the discrepancy is due to the inaccuracies in the potential function used in our MD simulation, since the Tersoff parameterization for ZnTe developed by Kanoun *et al.*[30] underestimates the elastic constants of bulk ZnTe. For the same reason, the bulk modulus for ZnTe from MD simulations shown in Fig. 5 is also underpredicted. The results also suggest that the toughness (opposite to rigidity) of ZnTe NWs, which is related to the surface under the stress–strain relation, does not vary considerably with the diameter.

The deformation behavior of a 20 nm diameter ZnTe NW including 444 676 united atoms is illustrated in Fig. 7. The specimen uniformly extends along the loading direction up to high strain levels and no significant structural changes are observed. Considerable disorders quickly develop along the specimen (Fig. 7c and d) at strain levels close to the ultimate tensile strength. The evolution of disorders along the specimen results in the formation of subsequent voids in the specimen which accordingly conclude in final brittle rupture. The Zn atoms' radial distribution function (RDF) of a NW at various strain levels is shown in Fig. 8: (a) for core atoms and (b) for surface atoms. An RDF describes how the average atomic density varies as a function of distance from a particular atom. At a strain level close to the rupture point, the shapes of RDF undergo considerable changes which provide evidence for the development of significant structural changes along the ZnTe NW. However, as the rupture occurs in the specimen, the RDF shapes turn out to be close to that of equilibrated structure. In both cases for core and surface atoms, the peaks in the RDF for the "after rupture" situation occur at almost the same radial distances as in the case of the equilibrated structure. This suggests the retrieval of original structure in ZnTe NWs after the failure, followed by some stabilized and localized disorders along the specimen. Interestingly, the RDFs of surface atoms are considerably close to those of core atoms at various deformation levels, and peaks in both cases occur at the same radial distances. This latter observation implies that the surface atom deformation behavior is similar to that for core atoms in the case of ZnTe NWs.

The Young's modulus size dependency of metallic[24,25] and ZnO[14] NWs has been attributed to reconstruction of surface atoms. This happens as a result of different stress status between the surface and core atoms at the equilibrium (zero stress) condition. In metals, the surface atoms are usually under tensile

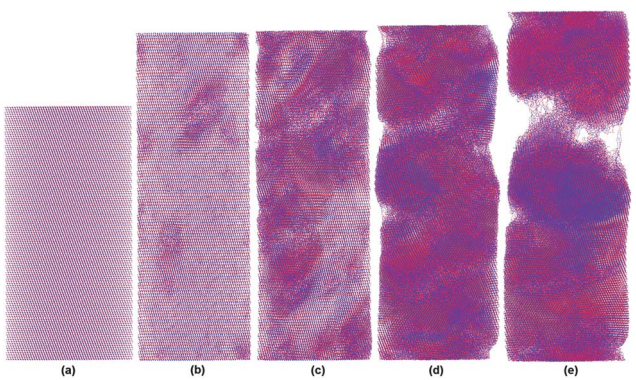

Fig. 7 The deformation behavior of a ZnTe NW with a diameter of 20 nm at different stages of loading: (a) initial configuration, (b) uniform extension along the loading direction up to the high strain levels, (c and d) development of disorders at strains close to the failure, and (e) final brittle failure.

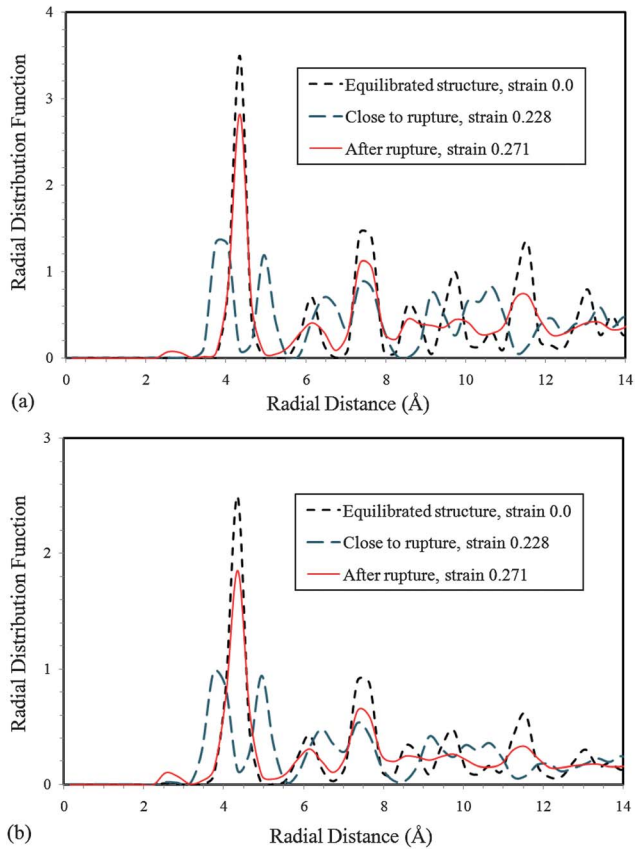

Fig. 8 Zn atoms' radial distribution functions (RDF) of a ZnTe NW at different strain levels: (a) for core atoms and (b) for surface atoms.

stress resulting in contraction of the NW at the equilibrium. Thus, the smaller metallic NW contracts more as a result of a higher ratio of surface to core atoms, which results in a higher Young's modulus.[26] In an opposite manner for ZnO, the surface atoms are in compression leading to overall expansion of the NW at equilibrium.[14] As mentioned before, in the case of ZnTe, the specimen was left to reach the zero stress along the axial (loading) direction before applying the loading condition. At the equilibrium point, we found that the surface atoms present negative stresses (compressive stress) which are neutralized by the positive stress (tensile stress) of the core atoms. These observations imply that, in a similar trend to ZnO, the surface atoms are in compression which results in overall expansion of the NW. The compressive state of surface atoms results in lower interatomic distances, which makes the surface atoms less stiff to tensile loading and more rigid for compression loading conditions. This finding was also verified by comparison of the stress–strain relation for the surface and core atoms, where the surface atoms present lower Young's modulus than the core atoms. This suggests a decrease in ZnTe NW Young's modulus with diameter, which is the case here only for diameters less than 7.5 nm. Similar to the metallic NWs,[24,25] the limited size dependency of ZnTe Young's modulus can be explained as a result of short range interactions. The interaction is short-ranged covalent type for ZnTe while the ionic bonding in ZnO is categorized as columbic long range. The material behavior is more localized in the short range interactions which means that reconstruction of surface atoms has negligible influence on the interaction of core atoms. This localized behavior is also observed from the RDF obtained from core and surface atoms at various deformation levels.

4. Conclusion

As tellurides of Zn, Cd, Pb and Bi have become popular for thermoelectric applications, a thorough characterization of their electrical and mechanical properties is needed.[33,34] We have investigated the size dependency of Young's modulus of ZnTe NWs here through bending tests in a TEM-AFM setup and also using computer simulations. The experimental method was used for NWs with diameters of 50–230 nm and the computational method was limited to NWs less than 20 nm in diameter due to computational efficiency. Neither of these two techniques show evidence of size dependency when the diameter exceeds 7.5 nm, with a limited dependency for smaller wires. The Young's modulus of ZnTe NWs is 63 ± 6 GPa and 55.5 ± 1 GPa, respectively, from the measurements and simulations. The ZnTe NWs are found to be flexible one-dimensional nanostructures and the results of this study will be useful for the design of various devices using these nanowires.

Acknowledgements

This work was supported by the World Class University program through the National Research Foundation of Korea funded by the Ministry of Education, Science and Technology under Project R31-2008-000-10100-0. RSY would like to acknowledge the funding support through the NSF-DMR Grant 0820884 and NSF-CMMI Grant 0926819.

References

1 Y. Zhu, C. Ke and H. D. Espinosa, Experimental techniques for the mechanical characterization of one dimensional nanostructures, *Exp. Mech.*, 2007, **47**, 7–24.
2 M. F. Yu, O. Lourie, M. J. Dyer, K. Moloni, T. F. Kelly and R. S. Ruoff, Strength and breaking mechanism of multiwalled carbon nanotubes under tensile load, *Science*, 2000, **287**, 637–640.
3 P. Poncharal, Z. L. Wang, D. Ugarte and W. A. De Heer, Electrostatic deflections and electromechanical resonances of carbon nanotubes, *Science*, 1999, **283**, 1513–1516.
4 R. P. Gao, Z. L. Wang, Z. Bai, W. A. de Heer, L. Dai and M. Gao, Nanomechanics of individual carbon nanotubes from pyrolytically grown arrays, *Phys. Rev. Lett.*, 2000, **85**, 622–625.
5 J. P. Salvetat, G. A. D. Briggs, J. M. Bonard, R. R. Basca, A. J. Kulik, T. Stöckli, N. A. Burnham and L. Forro, Elastic and shear moduli of single-walled carbon nanotube ropes, *Phys. Rev. Lett.*, 1999, **82**, 944–947.
6 D. A. Walters, L. M. Ericson, M. J. Casavant, J. Liu, D. T. Colbert, K. A. Smith and R. E. Smalley, Elastic strain of freely suspended single-wall carbon nanotube ropes, *Appl. Phys. Lett.*, 1999, **74**, 3803–3805.
7 M. Meyyappan and M. K. Sunkara, *Inorganic Nanowires: Properties, Characterization and Applications*, CRC Press, Boca Raton, FL, 2010.
8 E. W. Wong, P. E. Sheehan and C. M. Lieber, Nanobeam mechanics: elasticity, strength, and toughness of nanorods and nanotubes, *Science*, 1997, **277**, 1971–1975.
9 B. Wu, A. Heidelberg and J. J. Boland, Mechanical properties of ultrahigh-strength gold nanowires, *Nat. Mater.*, 2005, **4**, 525–529.
10 Y. Huang, X. Bai and Y. Zhang, *In situ* mechanical properties of individual ZnO nanowires and the mass measurement of nanoparticles, *J. Phys.: Condens. Matter*, 2006, **18**, L179–L184.
11 X. D. Bai, P. X. Gao, G. L. Wang and E. G. Wang, Dual-mode mechanical resonance of individual ZnO nanobelts, *Appl. Phys. Lett.*, 2003, **82**, 4806–4808.

12 C. Q. Chen, Y. Shi, Y. S. Zhang, J. Zhu and Y. J. Yan, Size dependence of Young's modulus in ZnO nanowires, *Phys. Rev. Lett.*, 2006, **96**, 075505.
13 Y. Zhu and H. D. Espinosa, An electromechanical material testing system for *in situ* electron microscopy and applications, *Proc. Natl. Acad. Sci. U. S. A.*, 2005, **102**, 14503–14508.
14 R. Agrawal, B. Peng, E. E. Gdoutous and H. D. Espinosa, Elasticity size effects in ZnO nanowires-a combined experimental-computational approach, *Nano Lett.*, 2008, **8**, 3668–3674.
15 K. Davami, D. Kang, J. S. Lee and M. Meyyappan, Synthesis of ZnTe nanostructures by vapor–liquid–solid technique, *Chem. Phys. Lett.*, 2011, **504**, 62.
16 H. M. Ghassemi, C. H. Lee, Y. K. Yap and R. S. Yassar, Real-time fracture detection of individual boron nitride nanotubes in severe cyclic deformation processes, *J. Appl. Phys.*, 2010, **108**, 024314.
17 A. S. Nishijima, T. Kisida and Y. Nakayam, Influence of force acting on side face of carbon nanotube in atomic force microscopy, *Jpn. J. Appl. Phys.*, 2000, **39**, 3724.
18 M. S. R. N. Kiran, S. Kshirasagar, M. Ghanashyam Krishna and S. P. Tewari, Structural, optical and nanomechanical properties of (111) oriented nanocrystalline ZnTe thin films, *Eur. Phys. J.: Appl. Phys.*, 2010, **51**, 10502.
19 M. Yamada, K. Yamamoto and K. Abe, Elastic and photoelastic constants of ZnTe measured by Brillouin scattering, *J. Phys. D: Appl. Phys.*, 1977, **10**, 1309.
20 B. H. Lee, Elastic constants of ZnTe and ZnSe between 77°–300° K, *J. Appl. Phys.*, 1970, **41**, 2984.
21 S. H. Park, J. S. Kim, J. H. Park, J. S. Lee, Y. K. Choi and O. M. Kwon, Molecular dynamics study on size-dependent elastic properties of silicon nanocantilevers, *Thin Solid Films*, 2005, **492**, 285–289.
22 A. Asthana, K. Momeni, A. Prasad, Y. K. Yap and R. S. Yassar, *In situ* observation of size-scale effects on the mechanical properties of ZnO nanowires, *Nanotechnology*, 2011, **22**, 265712.
23 F. Xu, Q. Qin, A. Mighra and Y. Zhu, Mechanical properties of ZnO nanowires under different loading modes, *Nano Res.*, 2010, **3**, 271–280.
24 J. K. Diao, K. Gall and M. L. Dunn, Surface-stress-induced phase transformation in metal nanowires, *Nat. Mater.*, 2003, **2**, 656–660.
25 J. K. Diao, K. Gall and M. L. Dunn, Surface stress driven reorientation of gold nanowires, *Phys. Rev. B: Condens. Matter Mater. Phys.*, 2004, **70**, 075413.
26 R. A. J. Kulkarni, M. Zhou and J. Qu, A semi-analytical method for quantifying the size-dependent elasticity of nanostructures, *Modell. Simul. Mater. Sci. Eng.*, 2008, **16**, 025002.
27 H. Liang, M. Upmanyu and H. Huang, Size-dependent elasticity of nanowires: nonlinear effects, *Phys. Rev. B: Condens. Matter Mater. Phys.*, 2005, **71**, 241403.
28 C. L. Hsin, W. Mai, Y. Gu, Y. Gao, C. T. Huang, Y. Liu, L. J. Chen and Z. L. Wang, Elastic properties and buckling of silicon nanowires, *Adv. Mater.*, 2008, **20**, 3919–3923.
29 S. Plimpton, Fast parallel algorithms for short-range molecular dynamics, *J. Comp. Physiol.*, 1995, **117**, 1.
30 M. B. Kanoun, A. E. Merad, H. Aourag, J. Cibert and G. Merad, Molecular-dynamics simulations of structural and thermodynamic properties of ZnTe using a three-body potential, *Solid State Sci.*, 2003, **5**, 1211.
31 H. Wang and W. Chu, Thermal conductivity of ZnTe investigated by molecular dynamics, *J. Alloys Compd.*, 2009, **485**, 488–492.
32 M. P. Allen and D. J. Tildesley, *Computer Simulation of Liquid*, Oxford Science, 1987.
33 K. Davami, H. M. Ghassemi, R. S. Yasser, J. S. Lee and M. Meyyappan, Thermal breakdown of ZnTe nanowires, *ChemPhysChem*, 2011, DOI: 10.1002/cphc.201100486.
34 K. Davami, H. M. Ghassemi, X. H. Sun, R. S. Yasser, J. S. Lee and M. Meyyappan, *In situ* observation of morphological change in CdTe nano- and submicron wires, *Nanotechnology*, 2011, **22**, 435204.